

RESEARCH

Open Access

OSTBC transmission in MIMO AF relaying with M -FSK modulation

Ha X Nguyen^{1*}, Chai Dai Truyen Thai² and Nguyen N Tran³

Abstract

This paper investigates orthogonal space-time block code (OSTBC) transmission for multiple-input multiple-output (MIMO) amplify-and-forward (AF) relaying networks composed of one source, K relays, and one destination and with M -ary frequency-shift keying (FSK) modulation. A non-coherent detection scheme is proposed and analyzed in a situation where the fading channels undergo temporal correlation. Specifically, by properly exploiting the implicit pilot-symbol-assist property of FSK transmission, the destination estimates the overall channels based on the linear minimum mean square error (LMMSE) estimation algorithm. It then utilizes the maximal ratio combining (MRC) to detect the transmitted information. An upper bound on the probability of errors is derived for a network with arbitrary numbers of transceiver antennas and relays. Based on the obtained bit error rate, the full achievable diversity order is verified. Simulation results are presented to show the validity of the analytical results.

Keywords: Cooperative diversity; Relay communications; Frequency-shift-keying; Fading channel; Amplify-and-forward protocol; Multiple-input multiple-output; Orthogonal space-time block codes

1 Introduction

Non-coherent transmission techniques have received a lot of attention due to their potential improvement in complexity by eliminating the need of channel state information at the receiver. Consequently, employing those non-coherent techniques is preferable in wireless relay networks since there are many wireless fading channels involved in the networks [1-4], which makes the task of channel estimation very complex and expensive to implement.

In recent years, much more research work has focused on non-coherent wireless relay networks [5-14], i.e., the wireless relay networks in which channel state information (CSI) is assumed to be unknown at the receivers (relays and destination). Among them, non-coherent amplify-and-forward (AF) has received more attention since it further puts a less processing burden on the relays due to the AF protocol [5-14]. However, only suboptimal non-coherent AF receivers have been studied due to the complicated deployment in practice [9,12]. Especially, when the channels undergo temporally correlated

Rayleigh flat fading, reference [13] is the only work to develop a detection scheme for non-coherent amplify-and-forward (AF) relay networks. It would be emphasized that all the abovementioned works assume that all nodes in the network are equipped with a single antenna.

Multiple-input multiple-output (MIMO) relaying techniques, which use multiple antennas at all nodes in the network, have been known to improve considerably performance in terms of data transmission rates as well as reliability over wireless channels. In particular, an exact ergodic capacity is analyzed and presented in [15], while the symbol error rate performance of orthogonal space-time block code (OSTBC) schemes in MIMO-AF relaying is studied in [16,17]. However, most existing works assume the availability of CSI of all the transmission links propagated by the received signals at the receivers to perform a detection [15-19]. Hence, non-coherent MIMO relaying networks are studied in this paper to make the MIMO relaying techniques more applicable. In fact, the work in [20] preliminarily develops a detection framework for multi-antenna AF relay networks. However, the work only considers a special network in which the source is equipped with two transmit antennas, the multiple relays and destination are equipped with a single antenna, and an Alamouti space-time block code is employed.

*Correspondence: ha.nguyen@ttu.edu.vn

¹School of Engineering, Tan Tao University, Tan Duc E-city, Duc Hoa, Long An, Vietnam

Full list of author information is available at the end of the article

This work studies a more generalized multi-antenna AF relay network, i.e., all the nodes in the network are equipped with multiple antennas. OSTBC is employed at the source to transmit a signal to the destination. Basically, the technique employed in this work is similar to that in [13,20]. By using the linear minimum mean square error (LMMSE) estimation algorithm, the destination first estimates the overall channels based on the pilot symbol inherent in frequency-shift keying (FSK) transmission. Then, it employs the maximal ratio combining (MRC) to detect the transmitted information. The main contribution of this paper is to develop a general framework for a network with arbitrary numbers of nodes and arbitrary numbers of transceiver antennas equipped at each node. Moreover, a unified upper-bound bit error rate (BER) expression is derived. It is further shown that the proposed detection scheme achieves a full diversity order.

The remainder of this paper is organized as follows. Section 2 describes the system model and detection framework. Section 3 derives an upper-bound on the BER when binary FSK (BFSK) is used. A full achievable diversity order is also shown in this section. Simulation results are presented in Section 4 to corroborate the analysis. Section 5 concludes the paper.

Notations: Superscripts $(\cdot)^*$, $(\cdot)^t$ and $(\cdot)^H$ stand for conjugate, transpose, and Hermitian transpose operations, respectively. $\text{Re}(x)$ takes the real part of a complex number x . For a random variable (RV) X , $f_X(\cdot)$ denotes its probability density function (pdf), and $\mathbb{E}_X\{\cdot\}$ denotes its expectation. $\mathcal{CN}(0, \sigma^2)$ denotes a circularly symmetric complex Gaussian random variable with variance σ^2 . $\mathbb{C}^{k \times 1}$ represents a $k \times 1$ vector where each element is a complex number. The gamma function is defined as $\Gamma(x) = \int_0^\infty \exp(-t)t^{x-1}dt$, $\text{Re}(x) > 0$. $J_0(x)$ is the zero-th order Bessel function of the first kind. The moment-generating function (MGF) of random variable X is denoted by $M_X(s)$, i.e., $M_X(s) = \mathbb{E}_X\{\exp(-sX)\}$. The discrete-time Dirac delta function is represented by $\delta[\cdot]$. The waveform of a signal is presented in a continuous form as $x(t)$. Meanwhile, the output of the matched filter of $x(t)$ is denoted by $x[k]$.

2 Orthogonal space-time AF relay systems with M-FSK modulation

2.1 System model

Consider a wireless relay network in which the source, denoted by node 0, communicates with the destination, denoted by node $K + 1$, with the assistance of K half-duplex relays, denoted by node i , $i = 1, \dots, K$, as illustrated in Figure 1. It is assumed that the K relays retransmit signals to the destination over orthogonal channels. All the nodes are MIMO devices, i.e., node i is equipped with N_i antennas. Assume that the transmit and receive antennas at a relay node are the same. An orthogonal

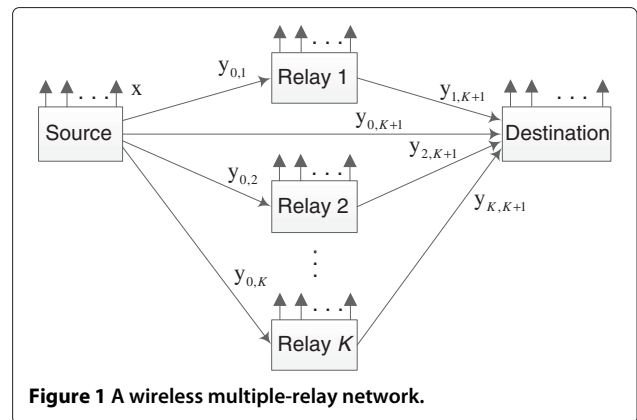


Figure 1 A wireless multiple-relay network.

space-time block code is employed at the source to transmit the signal to the destination. Fixed-gain AF protocol is employed at the relays.

The transmission protocol in this paper is built upon Protocol II [21]. In the first phase, i.e., T_c time slots, the source broadcasts an OSTBC designed for N_0 antennas to the relays and destination. In the second phase, i.e., the next $\sum_{i=1}^K N_i T_c$ time slots^a, the relays amplify the received signals and forward to the destination. The destination then estimates the overall channels of all the links from the source to the destination and performs a MRC with $(\sum_{i=1}^K N_i + 1) N_{K+1} T_c$ received signals for the final detection decision based on the estimated overall channels.

For convenience, let us adopt the convention that epoch k is a period of time to complete a signal transmission from the source to the destination. With the abovementioned transmission protocol, epoch k starts at $t = k(\sum_{i=1}^K N_i + 1) T_c T$ and ends at $(k + 1)(\sum_{i=1}^K N_i + 1) T_c T$ where T is the symbol duration (or time slot duration). The channel fading coefficient between the m th transmit antenna of node i and the n th receive antenna of node j at epoch k is denoted by $h_{<i,j>}^{<m,n>}[k]$. Those channel coefficients are modeled as circularly symmetric complex Gaussian random variables and assumed to be constant over $(\sum_{i=1}^K N_i + 1) T_c$ time slots but vary dependently every period of $(\sum_{i=1}^K N_i + 1) T_c$ time slots. The temporally correlated fading environment is modeled with the following Jake's autocorrelation:

$$\begin{aligned} \phi_{<i,j>}^{<m,n>}[p] &= \mathbb{E} \left\{ \left(h_{<i,j>}^{<m,n>}[p+q] \right)^* h_{<i,j>}^{<m,n>}[q] \right\} \\ &= \left(\sigma_{<i,j>}^{<m,n>} \right)^2 J_0 \left(2\pi f_{<i,j>}^{<m,n>} p \right) \end{aligned} \quad (1)$$

where $f_{<i,j>}^{<m,n>}$ and $\left(\sigma_{<i,j>}^{<m,n>} \right)^2$ are the maximum Doppler frequency and the average signal strength of the channel

corresponding to the connection between the m th transmit antenna of node i and the n th receive antenna of node j , respectively.

The received signal during the l th ($l = 1, \dots, T_c$) time slot of the first phase at the n th antenna of node j , $n = 1, \dots, N_i, j = 1, \dots, K + 1$, at epoch k is written as

$$y_{<0,j>}^{<n>,l}(t) = \sqrt{\frac{E_0}{N_0}} \sum_{m=1}^{N_0} h_{<0,j>}^{<m,n>} [k] x_{<j>}^l(t) + w_{<0,j>}^{<n>,l}(t), \quad t \in \mathbf{T}_{k,l} \quad (2)$$

where $\mathbf{T}_{k,l} = \left[k \left(\sum_{i=1}^K N_i + 1 \right) T_c T + (l-1)T, k \left(\sum_{i=1}^K N_i + 1 \right) T_c T + lT \right)$ denotes the interval of time slot l of epoch k , and $w_{<0,j>}^{<n>,l}(t)$ is the zero-mean additive white Gaussian noise (AWGN) at the n th antenna of node j with two-sided power spectral density (PSD) of $\kappa/2$ during the l th time slot. In the above expression, E_0 represents the average symbol energy available at the source and $x_{<j>}^l(t)$ is the transmitted waveform sent from the j th antenna of node 0 during time slot l . This waveform is chosen from an M -ary FSK constellation and therefore is written in complex baseband as

$$x_{<j>}^l(t) = \frac{1}{\sqrt{T}} \exp\left(\frac{i\pi t}{T}(2m - M - 1)\right), m = 1, \dots, M \quad (3)$$

The following amplifying factor is chosen at the n th antenna of relay node j before retransmitting:

$$\beta_{<j>}^{<n>} = \sqrt{\frac{E_j/N_j}{\mathbb{E}\{|y_{<j>}^{<n>,l}(t)|^2\}}} = \sqrt{\frac{E_j/N_j}{E_0/N_0 \sum_{m=1}^{N_0} (\sigma_{<0,j>}^{<m,n>})^2 + \kappa}}, \quad (4)$$

where E_j is the average transmitted symbol energy allocated to node j . The received signal at the g th antenna of the destination via the n th antenna of relay node j at epoch k , i.e., during the time interval $t \in \mathbf{T}_{k,l}$, $l = T_c + 1, T_c + 2, \dots, \left(\sum_{i=1}^K N_i + 1 \right) T_c$, can be written as

$$\begin{aligned} y_{<j,K+1>}^{<n,g>,l}(t) &= \beta_{<j>}^{<n>} h_{<j,K+1>}^{<n,g>} [k] y_{<0,j>}^{<n>,l-\left(\sum_{i=1}^{j-1} N_i + 1\right) T_c} \\ &\quad \times \left(t - \left(l - \left(\sum_{i=1}^{j-1} N_i + 1 \right) T_c \right) T \right) \\ &\quad + w_{<j,K+1>}^{<n,g>,l}(t) \\ &= \sum_{m=1}^{N_0} \beta_{<j>}^{<n>} \sqrt{E_0} h_{<0,j,K+1>}^{<m,n,g>} [k] x_{<j>}^{l-\left(\sum_{i=1}^{j-1} N_i + 1\right) T_c} \\ &\quad \times \left(t - \left(l - \left(\sum_{i=1}^{j-1} N_i + 1 \right) T_c \right) T \right) \\ &\quad + w_{<0,j,K+1>}^{<n,g>,l}(t), \end{aligned} \quad (5)$$

where $h_{<0,j,K+1>}^{<m,n,g>} [k] = h_{<0,j>}^{<m,n>} [k] h_{<j,K+1>}^{<n,g>} [k]$ is the overall channels from the m th antenna of the source to the g th antenna of the destination via the n th antenna of node j at epoch k . The waveform $w_{<0,j,K+1>}^{<n,g>,l}(t) = \beta_{<j>}^{<n>} h_{<j,K+1>}^{<n,g>} [k] w_{<0,j>}^{<n>,l-\left(\sum_{i=1}^{j-1} N_i + 1\right) T_c} \left(t - \left(l - \left(\sum_{i=1}^{j-1} N_i + 1 \right) T_c \right) T \right) + w_{<j,K+1>}^{<n,g>,l}(t)$ is the total additive noise corrupting the received signal. The noise $w_{<j,K+1>}^{<n,g>,l}(t)$ is also a zero-mean AWGN with two-side PSD of $\kappa/2$.

It should be noted that the proposed transmission scheme typically suffers a certain throughput loss because it requires $T_c \left(\sum_{i=1}^K N_i + 1 \right)$ time slot to complete a transmission of $\log M$ bits. However, this is due to the decoding rule implemented at the destination. In practice, one shall design to accommodate the system requirements by adjusting the trade-off between the complexity, throughput, and bit error rate.

In what follows, the abovementioned two-step detection is presented in detail. The estimation of the overall channels of all the links from the source to the destination is described first, followed by the detection decision by using a MRC.

2.2 Channel estimation

The destination correlates the received signals in (2) and (5) with the following sum waveform $r(t)$ to estimate the overall channels [13,22]:

$$r(t) = \sum_{l=1}^{\frac{M}{2}} \frac{2}{\sqrt{T}} \cos\left((2l-1)\frac{\pi t}{T}\right) \quad (6)$$

The output of the correlators can be stacked and reorganized as^b

$$y_{<0,K+1>}^{(E)} = \sqrt{\frac{E_0}{N_0}} X_{<0,K+1>}^{(E)} \mathbf{h}_{<0,K+1>} + \mathbf{w}_{<0,K+1>}^{(E)}, \quad (7)$$

$$y_{<j,K+1>}^{(E)} = \sqrt{\frac{E_0}{N_0}} X_{<j,K+1>}^{(E)} \mathbf{h}_{<0,j,K+1>} + \mathbf{w}_{<j,K+1>}^{(E)}, j = 1, \dots, K \quad (8)$$

where the channel vectors $\mathbf{h}_{<0,K+1>} \in \mathbb{C}^{N_0 N_{K+1} \times 1}$ and $\mathbf{h}_{<0,j,K+1>} \in \mathbb{C}^{N_0 N_j N_{K+1} \times 1}$ are

$$\begin{aligned} \mathbf{h}_{<0,K+1>} &= \left(h_{<0,K+1>}^{<1,1>} \cdots h_{<0,K+1>}^{<N_0,1>} h_{<0,K+1>}^{<1,2>} \cdots \right. \\ &\quad \left. h_{<0,K+1>}^{<N_0,N_{K+1}>} \right)^t, \end{aligned} \quad (9)$$

$$\begin{aligned} \mathbf{h}_{<0,j,K+1>} &= \left(h_{<0,j,K+1>}^{<1,1,1>} \cdots h_{<0,j,K+1>}^{<N_0,1,1>} h_{<0,j,K+1>}^{<1,1,2>} \cdots \right. \\ &\quad \left. h_{<0,j,K+1>}^{<N_0,1,N_{K+1}>} h_{<0,j,K+1>}^{<1,2,1>} \cdots h_{<0,j,K+1>}^{<N_0,N_j,N_{K+1}>} \right)^t. \end{aligned} \quad (10)$$

The noise vectors $w_{<0,K+1>}^{(E)} \in \mathbb{C}^{N_{K+1}T_c \times 1}$ and $w_{<j,K+1>}^{(E)} \in \mathbb{C}^{N_j N_{K+1} T_c \times 1}$ are

$$w_{<0,K+1>}^{(E)} = \left(w_{<0,K+1>}^{<1>,1} \cdots w_{<0,K+1>}^{<1>,T_c} \ w_{<0,K+1>}^{<2>,1} \cdots w_{<0,K+1>}^{<N_{K+1}>,T_c} \right)^t, \quad (11)$$

$$w_{<j,K+1>}^{(E)} = \left(w_{<j,K+1>}^{<1,1>,1} \cdots w_{<j,K+1>}^{<1,1>,T_c} \ w_{<j,K+1>}^{<1,2>,1} \cdots w_{<j,K+1>}^{<1,N_{K+1}>,T_c} \ w_{<j,K+1>}^{<2,1>,1} \cdots w_{<j,K+1>}^{<N_j,N_{K+1}>,T_c} \right)^t. \quad (12)$$

Meanwhile, the signal vectors $y_{<0,K+1>}^{(E)} \in \mathbb{C}^{N_{K+1}T_c \times 1}$ and $y_{<j,K+1>}^{(E)} \in \mathbb{C}^{N_j N_{K+1} T_c \times 1}$ are

$$y_{<0,K+1>}^{(E)} = \left(y_{<0,K+1>}^{<1>,1} \cdots y_{<0,K+1>}^{<1>,T_c} \ y_{<0,K+1>}^{<2>,1} \cdots y_{<0,K+1>}^{<N_{K+1}>,T_c} \right)^t, \quad (13)$$

$$y_{<j,K+1>}^{(E)} = \left(y_{<j,K+1>}^{<1,1>,1} \cdots y_{<j,K+1>}^{<1,1>,T_c} \ y_{<j,K+1>}^{<1,2>,1} \cdots y_{<j,K+1>}^{<1,N_{K+1}>,T_c} \ y_{<j,K+1>}^{<2,1>,1} \cdots y_{<j,K+1>}^{<N_j,N_{K+1}>,T_c} \right)^t. \quad (14)$$

On the other hand, $X_{<0,K+1>}^{(E)}$ and $X_{<j,K+1>}^{(E)}$ are defined as two N_{K+1} and $N_j N_{K+1}$ block diagonal matrices, respectively, i.e.,

$$X_{<0,K+1>}^{(E)} = \text{diag} \left\{ \underbrace{X, X, \dots, X}_{N_{K+1} \text{ elements}} \right\}, \quad (15)$$

$$X_{<j,K+1>}^{(E)} = \text{diag} \left\{ \underbrace{\beta_{<j>}^{<1>} X, \beta_{<j>}^{<2>} X, \dots, \beta_{<j>}^{<N_j>} X, \beta_{<j>}^{<N_j>} X, \dots, \beta_{<j>}^{<N_j>} X}_{N_{K+1} \text{ elements}} \right\}, \quad (16)$$

where block X is the $T_c \times N_0$ matrix code with the elements of 1 or -1 . For example, if an Alamouti code is employed at the source, then $X = \begin{pmatrix} 1 & 1 \\ -1 & 1 \end{pmatrix}$.

Using LMMSE estimators, the LMMSE estimations of $h_{<0,K+1>}[k]$ and $h_{<0,i,K+1>}[k]$ can be obtained as follows [23-25]:

$$\hat{h}_{<0,K+1>} = \Psi_{h_{<0,K+1>} \bar{y}_{<0,K+1>}^{(E)}} \left(\Phi_{\bar{y}_{<0,K+1>} \bar{y}_{<0,K+1>}^{(E)}} \right)^{-1} \bar{y}_{<0,K+1>}^{(E)} \quad (17)$$

$$\hat{h}_{<0,j,K+1>} = \Psi_{h_{<0,j,K+1>} \bar{y}_{<0,j,K+1>}^{(E)}} \left(\Phi_{\bar{y}_{<0,j,K+1>} \bar{y}_{<0,j,K+1>}^{(E)}} \right)^{-1} \bar{y}_{<0,j,K+1>}^{(E)}, \quad j = 1, \dots, K \quad (18)$$

In the above expressions, $\bar{y}_{<0,K+1>}^{(E)} \in \mathbb{C}^{(2P+1)N_{K+1}T_c \times 1}$ and $\bar{y}_{<0,j,K+1>}^{(E)} \in \mathbb{C}^{(2P+1)N_j N_{K+1} T_c \times 1}$, $j = 1, \dots, K$, are formed by stacking $2P + 1$ consecutive vectors $y_{<0,K+1>}^{(E)}[k + l]$ and $y_{<0,j,K+1>}^{(E)}[k + l]$, $l = -P, \dots, P$, respectively. $\Psi_{h \bar{y}^{(E)}}$ denotes the correlation matrix between h and $\bar{y}^{(E)}$. $\Phi_{\bar{y}^{(E)} \bar{y}^{(E)}}$ is the auto-correlation matrix of $\bar{y}^{(E)}$. As mentioned in [13], there is a trade-off between complexity and performance, i.e., increasing P may improve the performance but also increase the complexity. Additional (implicit) pilot symbols will increase the size of the matrices; therefore, it is expected to have a higher complexity to deal with matrix computations.

The matrices $\Psi_{h_{<0,K+1>} \bar{y}_{<0,K+1>}^{(E)}}$ and $\Psi_{h_{<0,j,K+1>} \bar{y}_{<0,j,K+1>}^{(E)}}$ are computed, respectively, as follows:

$$\Psi_{h_{<0,K+1>} \bar{y}_{<0,K+1>}^{(E)}} = \left(\sqrt{\frac{E_0}{N_0}} \Theta_{<0,K+1>}[k - P] \quad \sqrt{\frac{E_0}{N_0}} \Theta_{<0,K+1>}[k - P + 1] \quad \dots \quad \sqrt{\frac{E_0}{N_0}} \Theta_{<0,K+1>}[k + P] \right), \quad (19)$$

$$\Psi_{h_{<0,j,K+1>} \bar{y}_{<0,j,K+1>}^{(E)}} = \left(\sqrt{\frac{E_0}{N_0}} \Theta_{<0,j,K+1>}[k - P] \quad \sqrt{\frac{E_0}{N_0}} \Theta_{<0,j,K+1>}[k - P + 1] \quad \dots \quad \sqrt{\frac{E_0}{N_0}} \Theta_{<0,j,K+1>}[k + P] \right), \quad (20)$$

where

$$\Theta_{<0,K+1>}[l] = \text{diag} \left\{ \phi_{<0,K+1>}^{<1,1>}[l], \phi_{<0,K+1>}^{<2,1>}[l], \dots, \phi_{<0,K+1>}^{<N_0,N_{K+1}>}[l] \right\} \left(X_{<0,K+1>}^{(E)} \right)^t, \quad (21)$$

$$\Theta_{<0,j,K+1>}[l] = \text{diag} \left\{ \phi_{<0,j,K+1>}^{<1,1,1>}[l], \dots, \phi_{<0,j,K+1>}^{<N_0,1,1>}[l], \dots, \phi_{<0,j,K+1>}^{<N_0,N_j,N_{K+1}>}[l] \right\} \left(X_{<0,j,K+1>}^{(E)} \right)^t, \quad (22)$$

where $\phi_{<0,j,K+1>}^{<m,n,g>}[l]$ is the auto-correlation function of the overall channel $h_{<0,j,K+1>}^{<m,n,g>}$. One has [23]

$$\phi_{<0,j,K+1>}^{<m,n,g>}[l] = \phi_{<0,j>}^{<m,n>}[l] \phi_{<j,K+1>}^{<n,g>}[l] = \left(\sigma_{<0,j>}^{<m,n>} \right)^2 \left(\sigma_{<j,K+1>}^{<n,g>} \right)^2 J_0 \left(2\pi f_{<0,j>}^{<m,n>} l \right) J_0 \left(2\pi f_{<j,K+1>}^{<n,g>} l \right) \quad (23)$$

Meanwhile, the matrices $\Phi_{\bar{Y}_{<0,K+1>}^{(E)} \bar{Y}_{<0,K+1>}^{(E)}}$ and $\Phi_{\bar{Y}_{<0,j,K+1>}^{(E)} \bar{Y}_{<0,j,K+1>}^{(E)}}$ can be presented as $\Phi_{\bar{Y}_{<0,K+1>}^{(E)} \bar{Y}_{<0,K+1>}^{(E)}}$ = $\left[(\mathbf{S}_{<0,K+1>})_{p,q} \right]_{(2P+1) \times (2P+1)}$ and $\Phi_{\bar{Y}_{<0,j,K+1>}^{(E)} \bar{Y}_{<0,j,K+1>}^{(E)}}$ = $\left[(\mathbf{S}_{<0,j,K+1>})_{p,q} \right]_{(2P+1) \times (2P+1)}$ where $(\mathbf{S}_{<0,K+1>})_{p,q}$ = $\left(\text{diag} \left\{ \Lambda_{<0,K+1>}^{<1>}, \Lambda_{<0,K+1>}^{<2>}, \dots, \Lambda_{<0,K+1>}^{<N_{K+1}>} \right\} \right)_{p,q}$, $(\mathbf{S}_{<0,j,K+1>})_{p,q}$ = $\left(\text{diag} \left\{ \Lambda_{<0,j,K+1>}^{<1>}, \Lambda_{<0,j,K+1>}^{<2>}, \dots, \Lambda_{<0,j,K+1>}^{<N_{K+1}>} \right\} \right)_{p,q}$ and

$$\left(\Lambda_{<0,K+1>}^{<g>} \right)_{p,q} = X \text{diag} \left\{ \frac{E_0}{N_0} \phi_{<0,K+1>}^{<1,g>}[p-q], \dots, \frac{E_0}{N_0} \phi_{<0,K+1>}^{<N_0,g>}[p-q] \right\} X^t + MN_0 \delta[p-q] I_{N_0 \times N_0}, \quad (24)$$

$$\left(\Lambda_{<0,j,K+1>}^{<g>} \right)_{p,q} = \text{diag} \left\{ \left(\Lambda_{<0,j,K+1>}^{<1,g>} \right)_{p,q}, \left(\Lambda_{<0,j,K+1>}^{<2,g>} \right)_{p,q}, \dots, \left(\Lambda_{<0,j,K+1>}^{<N_j,g>} \right)_{p,q} \right\}, \quad (25)$$

$$\begin{aligned} \left(\Lambda_{<0,j,K+1>}^{<n,g>} \right)_{p,q} &= X \text{diag} \left\{ \left(\beta_{<j>}^{<n>} \right)^2 \frac{E_0}{N_0} \phi_{<0,j,K+1>}^{<1,n,g>}[p-q], \dots, \left(\beta_{<j>}^{<n>} \right)^2 \frac{E_0}{N_0} \phi_{<0,j,K+1>}^{<N_0,n,g>}[p-q] \right\} X^t \\ &+ \left(\left(\beta_{<j>}^{<n>} \sigma_{<j,K+1>}^{<n,g>} \right)^2 MN_0 \delta[n-m] + MN_0 \delta[p-q] \right) I_{N_0 \times N_0}, \end{aligned} \quad (26)$$

where $g = 1, \dots, N_{K+1}$ and $n = 1, \dots, N_j$.

The estimation errors $e_{<0,K+1>}[k] = h_{<0,K+1>}[k] - \hat{h}_{<0,K+1>}[k]$ and $e_{<0,j,K+1>}[k] = h_{<0,j,K+1>}[k] - \hat{h}_{<0,j,K+1>}[k]$ are zero-mean with covariance matrices given as [25]

$$\mathbf{C}_{e_{<0,K+1>} e_{<0,K+1>}} = \mathbf{C}_{h_{<0,K+1>} h_{<0,K+1>}} - \Psi_{h_{<0,K+1>} \bar{Y}_{<0,K+1>}^{(E)}} \left(\Phi_{\bar{Y}_{<0,K+1>}^{(E)} \bar{Y}_{<0,K+1>}^{(E)}}$$

$$\begin{aligned} \mathbf{C}_{e_{<0,j,K+1>} e_{<0,j,K+1>}} &= \mathbf{C}_{h_{<0,j,K+1>} h_{<0,j,K+1>}} - \Psi_{h_{<0,j,K+1>} \bar{Y}_{<0,j,K+1>}^{(E)}} \left(\Phi_{\bar{Y}_{<0,j,K+1>}^{(E)} \bar{Y}_{<0,j,K+1>}^{(E)}}$$
 \\ &\times \Psi_{h_{<0,j,K+1>} \bar{Y}_{<0,j,K+1>}^{(E)}}^H, \quad j = 1, \dots, K \end{aligned} \quad (28)

It is clear that $\mathbf{C}_{e_{<0,K+1>} e_{<0,K+1>}}$ and $\mathbf{C}_{e_{<0,j,K+1>} e_{<0,j,K+1>}}$ are diagonal matrices. Let $\left(\tilde{\sigma}_{<0,K+1>}^{<m,n>} \right)^2$ and $\left(\tilde{\sigma}_{<0,j,K+1>}^{<m,n,g>} \right)^2$ be the variances of the estimation errors $e_{<0,K+1>}^{<m,n>}[k] = h_{<0,K+1>}^{<m,n>}[k] - \hat{h}_{<0,K+1>}^{<m,n>}[k]$ and $e_{<0,j,K+1>}^{<m,n,g>}[k] = h_{<0,j,K+1>}^{<m,n,g>}[k] - \hat{h}_{<0,j,K+1>}^{<m,n,g>}[k]$, respectively, then one has $\left(\tilde{\sigma}_{<0,K+1>}^{<m,n>} \right)^2 = \left[\mathbf{C}_{e_{<0,K+1>} e_{<0,K+1>}} \right]_{(n-1)N_0+m, (n-1)N_0+m}$ and $\left(\tilde{\sigma}_{<0,j,K+1>}^{<m,n,g>} \right)^2 = \left[\mathbf{C}_{e_{<0,j,K+1>} e_{<0,j,K+1>}} \right]_{((n-1)N_{K+1}+(g-1)N_0+m, ((n-1)N_{K+1}+(g-1)N_0+m)}$ where $[\mathbf{A}]_{i,i}$ represents the i th diagonal element of matrix \mathbf{A} .

2.3 Data detection

The destination correlates the received waveforms in (2) and (5) with the following vector $x(t)$ to detect the transmitted data:

$$x(t) = \left[x_1^*(t) \ x_2^*(t) \ \dots \ x_M^*(t) \right]^t. \quad (29)$$

The outputs of the correlators can be written as

$$y_{<0,K+1>}^{<n>,l}[k] = \sqrt{\frac{E_0}{N_0}} \sum_{m=1}^{N_0} \left(\hat{h}_{<0,K+1>}^{<m,n>}[k] + e_{<0,K+1>}^{<m,n>}[k] \right) x_{<m>}^l[k] + w_{<0,j>}^{<n>,l}[k], \quad t \in \mathbf{T}_{k,l} \quad (30)$$

$$y_{<j,K+1>}^{<n,g>,l}[k] = \sum_{m=1}^{N_0} \beta_{<j>}^{<n>} \sqrt{\frac{E_0}{N_0}} \left(\hat{h}_{<0,j,K+1>}^{<m,n,g>}[k] + e_{<0,j,K+1>}^{<m,n,g>}[k] \right) x_{<m>}^l[k] + w_{<0,j,K+1>}^{<n,g>,l}[k], \quad (31)$$

where $\mathbf{x}_{<m>}^l[k]$ is the $M \times 1$ vector that represents the transmit symbol from the m th antenna of node 0 at epoch k . Note that $\mathbf{x}_{<m>}^l[k]$ has 1 at an element and 0 at others. The elements of noise vectors $\mathbf{w}_{<0,j>}^{<n>,l}[k]$ and $\mathbf{w}_{<0,j,K+1>}^{<n,g>,l}[k]$ with size $M \times 1$ are i.i.d. zero-mean random variables with variance κ and $\left(\left(\beta_{<i>}^{<n>} \sigma_{<j,K+1>}^{<n,g>} \right)^2 + 1 \right) \kappa$, respectively.

By using the property of complex orthogonal designs, one can stack and rewrite the input/output relations as

$$\begin{pmatrix} \mathbf{y}_{<0,K+1>}^{<1>} \\ \mathbf{y}_{<0,K+1>}^{<2>} \\ \vdots \\ \mathbf{y}_{<0,K+1>}^{<N_{K+1}>} \end{pmatrix} = \sqrt{\frac{E_0}{N_0}} \begin{pmatrix} \hat{\mathbf{H}}_{<0,K+1>}^{<1>} \\ \hat{\mathbf{H}}_{<0,K+1>}^{<2>} \\ \vdots \\ \hat{\mathbf{H}}_{<0,K+1>}^{<N_{K+1}>} \end{pmatrix} \mathbf{x} + \sqrt{\frac{E_0}{N_0}} \begin{pmatrix} \mathbf{E}_{<0,K+1>}^{<1>} \\ \mathbf{E}_{<0,K+1>}^{<2>} \\ \vdots \\ \mathbf{E}_{<0,K+1>}^{<N_{K+1}>} \end{pmatrix} \mathbf{x} + \begin{pmatrix} \mathbf{w}_{<0,K+1>}^{<1>} \\ \mathbf{w}_{<0,K+1>}^{<2>} \\ \vdots \\ \mathbf{w}_{<0,K+1>}^{<N_{K+1}>} \end{pmatrix}, \quad (32)$$

$$\begin{pmatrix} \mathbf{y}_{<0,j,K+1>}^{<n,1>} \\ \mathbf{y}_{<0,j,K+1>}^{<n,2>} \\ \vdots \\ \mathbf{y}_{<0,j,K+1>}^{<n,N_{K+1}>} \end{pmatrix} = \beta_{<j>}^{<n>} \sqrt{\frac{E_0}{N_0}} \begin{pmatrix} \hat{\mathbf{H}}_{<0,j,K+1>}^{<n,1>} \\ \hat{\mathbf{H}}_{<0,j,K+1>}^{<n,2>} \\ \vdots \\ \hat{\mathbf{H}}_{<0,j,K+1>}^{<n,N_{K+1}>} \end{pmatrix} \mathbf{x} + \beta_{<j>}^{<n>} \sqrt{\frac{E_0}{N_0}} \begin{pmatrix} \mathbf{E}_{<0,j,K+1>}^{<n,1>} \\ \mathbf{E}_{<0,j,K+1>}^{<n,2>} \\ \vdots \\ \mathbf{E}_{<0,j,K+1>}^{<n,N_{K+1}>} \end{pmatrix} \mathbf{x} + \begin{pmatrix} \mathbf{w}_{<0,j,K+1>}^{<n,1>} \\ \mathbf{w}_{<0,j,K+1>}^{<n,2>} \\ \vdots \\ \mathbf{w}_{<0,j,K+1>}^{<n,N_{K+1}>} \end{pmatrix}, \quad \begin{matrix} j = 1, \dots, K \\ n = 1, \dots, N_j \end{matrix} \quad (33)$$

where $\mathbf{y}_{<0,K+1>}^{<g>} = \left(\tilde{\mathbf{y}}_{<0,K+1>}^{<g>,1} \dots \tilde{\mathbf{y}}_{<0,K+1>}^{<g>,T_c} \right)^t \in \mathbb{C}^{MT_c \times 1}$ and $\mathbf{y}_{<0,j,K+1>}^{<n,g>} = \left(\tilde{\mathbf{y}}_{<0,j,K+1>}^{<n,g>,1} \dots \tilde{\mathbf{y}}_{<0,j,K+1>}^{<n,g>,T_c} \right)^t \in \mathbb{C}^{MT_c \times 1}$, $g = 1, \dots, N_{K+1}$, represent the output of the correlators at the g th antenna of the destination. Similarly, $\mathbf{w}_{<0,K+1>}^g = \left(\tilde{\mathbf{w}}_{<0,K+1>}^{<g>,1} \dots \tilde{\mathbf{w}}_{<0,K+1>}^{<g>,T_c} \right)^t \in \mathbb{C}^{MT_c \times 1}$ and $\mathbf{w}_{<0,j,K+1>}^{<n,g>} = \left(\tilde{\mathbf{w}}_{<0,j,K+1>}^{<n,g>,1} \dots \tilde{\mathbf{w}}_{<0,j,K+1>}^{<n,g>,T_c} \right)^t \in \mathbb{C}^{MT_c \times 1}$ are the noise vectors. Note that $\tilde{\mathbf{y}}_{<0,K+1>}^{<g>,l} = \mathbf{y}_{<0,K+1>}^{<g>,l}$ or $\tilde{\mathbf{y}}_{<0,K+1>}^{<g>,l} = \left(\mathbf{y}_{<0,K+1>}^{<g>,l} \right)^*$ depends on the structure of OSTBCs. It is similar to $\tilde{\mathbf{y}}_{<0,j,K+1>}^{<n,g>,l}$, $\tilde{\mathbf{e}}_{<0,K+1>}^{<g>,l}$ and $\tilde{\mathbf{e}}_{<0,j,K+1>}^{<n,g>,l} \cdot \hat{\mathbf{H}}_{<0,K+1>}^g$ (or $\mathbf{E}_{<0,K+1>}^g$) and $\hat{\mathbf{H}}_{<0,j,K+1>}^{<n,g>}$ (or $\mathbf{E}_{<0,j,K+1>}^{<n,g>}$) denote the $MT_c \times MC$ matrices containing estimated channel gains (or channel estimation errors). Note that the matrices are uniquely obtained from any OSTBC. For example, for an Alamouti code employed at the source, the corresponding channel matrices will be

$$\hat{\mathbf{H}}_{<0,K+1>}^{<g>} = \begin{pmatrix} \text{diag} \left\{ \hat{h}_{<0,K+1>}^{<1,g>}, \dots, \hat{h}_{<0,K+1>}^{<1,g>} \right\} & \text{diag} \left\{ \hat{h}_{<0,K+1>}^{<2,g>}, \dots, \hat{h}_{<0,K+1>}^{<2,g>} \right\} \\ \text{diag} \left(\left\{ \hat{h}_{<0,K+1>}^{<2,g>}, \dots, \hat{h}_{<0,K+1>}^{<2,g>} \right\} \right)^* & \text{diag} \left(- \left\{ \hat{h}_{<0,K+1>}^{<1,g>}, \dots, \hat{h}_{<0,K+1>}^{<1,g>} \right\} \right)^* \end{pmatrix} \quad (34)$$

$$\hat{\mathbf{H}}_{<0,j,K+1>}^{<n,g>} = \begin{pmatrix} \text{diag} \left\{ \hat{h}_{<0,j,K+1>}^{<1,n,g>}, \dots, \hat{h}_{<0,j,K+1>}^{<1,n,g>} \right\} & \text{diag} \left\{ \hat{h}_{<0,j,K+1>}^{<2,n,g>}, \dots, \hat{h}_{<0,j,K+1>}^{<2,n,g>} \right\} \\ \text{diag} \left(\left\{ \hat{h}_{<0,j,K+1>}^{<2,n,g>}, \dots, \hat{h}_{<0,j,K+1>}^{<2,n,g>} \right\} \right)^* & \text{diag} \left(- \left\{ \hat{h}_{<0,j,K+1>}^{<1,n,g>}, \dots, \hat{h}_{<0,j,K+1>}^{<1,n,g>} \right\} \right)^* \end{pmatrix} \quad (35)$$

Lastly the vector $\mathbf{x}[k]$ is defined as

$$\mathbf{x}[k] = \begin{pmatrix} \mathbf{x}_1[k] \\ \vdots \\ \mathbf{x}_C[k] \end{pmatrix} \quad (36)$$

where $\mathbf{x}_c[k]$, $c = 1, \dots, C$ is the $M \times 1$ vector that represents the c th data symbol that enters the OSTBC encoder at epoch k . Note that $\mathbf{x}_c[k]$ is a unit vector.

Giving the estimated (overall) channels, the maximum signal-to-noise ratio (SNR) detector at the destination is of the following form

$$\mathbf{r}[k] = \sum_{g=1}^{N_{K+1}} \varepsilon_{<0,K+1>}^{<g>} \left(\hat{\mathbf{H}}_{<0,K+1>}^{<g>} \right)^H [k] \mathbf{y}_{<0,K+1>}^g [k] + \sum_{j=1}^K \sum_{g=1}^{N_{K+1}} \sum_{n=1}^{N_j} \varepsilon_{<j,K+1>}^{<n,g>} \left(\hat{\mathbf{H}}_{<0,j,K+1>}^{<n,g>} \right)^H [k] \mathbf{y}_{<j,K+1>}^{<n,g>} [k], \quad (37)$$

where the combining weights are

$$\varepsilon_{<0,K+1>}^{<g>} = \left(\frac{E_0}{N_0} \sum_{m=1}^{N_0} \left(\tilde{\sigma}_{<0,K+1>}^{<m,g>} \right)^2 + N_0 \kappa \right)^{-1} \tag{38}$$

$$\varepsilon_{<j,K+1>}^{<n,g>} = \left(\left(\beta_{<j>}^{<n>} \right)^2 \frac{E_0}{N_0} \sum_{m=1}^{N_0} \left(\tilde{\sigma}_{<0,j>,K+1}^{<m,n,g>} \right)^2 + N_0 \left(\beta_{<j>}^{<n>} \right)^2 \left(\sigma_{<j,K+1>}^{<n,g>} \right)^2 \kappa + N_0 \kappa \right)^{-1} \tag{39}$$

Finally, due to the orthogonal property of OSTBCs, the transmitted symbols are decided by

$$\left(\hat{m}, \hat{x}_c[k] \right) = \arg \max_{m=1, \dots, M} \text{Re} \left(r_{m+cM}[k] \right), \quad c = 1, \dots, C \tag{40}$$

where $r_i[k]$ is the i th element of the $MC \times 1$ vector $\mathbf{r}[k]$. $\hat{x}_c[k]$ is a $M \times 1$ unit vector with 1 at the m th element, i.e., the c th transmit waveform that enters the OSTBC encoder is decoded as using the m th M -FSK tone's frequency.

3 Upper bound on BER performance and diversity order

Naturally, the exact BER performance analysis of AF systems is difficult due to the non-Gaussian property of the noises in (33). Therefore, in this section, an upper bound on the BER is obtained by assuming that the noise is Gaussian [13].

Since the decision rule in (40) is equivalent to the symbol-wise decision rule, i.e., each transmitted symbol can be decoded independently, the instantaneous SNR at the combiner's output can be written as

$$\gamma = \sum_{g=1}^{N_{K+1}} \hat{\gamma}_{<0,K+1>}^{<g>} + \sum_{j=1}^K \sum_{n=1}^{N_j} \hat{\gamma}_{<j,K+1>}^n \tag{41}$$

where

$$\hat{\gamma}_{<0,K+1>}^{<g>} = \frac{E_0}{N_0} \varepsilon_{<0,K+1>}^{<g>} \left(\sum_{m=1}^{N_0} \left| \hat{h}_{<0,K+1>}^{<m,g>} \right|^2 \right) \tag{42}$$

$$\hat{\gamma}_{<j,K+1>}^n = \sum_{g=1}^{N_{K+1}} \frac{E_0}{N_0} \left(\beta_{<j>}^{<n>} \right)^2 \varepsilon_{<j,K+1>}^{<n,g>} \left(\sum_{m=1}^{N_0} \left| \hat{h}_{<0,j>,K+1}^{<m,n,g>} \right|^2 \right) \tag{43}$$

To simplify our analysis, we assume that BFSK is employed at the source, i.e., $M = 2$ and the average signal strength between any two antennas of two particular nodes is identical, i.e., $\left(\sigma_{<i,j>}^{<m,n>} \right)^2 = \left(\sigma_{<i,j>} \right)^2, i = 1, \dots, K$. It means that the average signal strength between any two antennas of the source-destination link via a relay is also identical, i.e., $\left(\sigma_{<0,j>,K+1}^{<m,n,g>} \right)^2 = \left(\sigma_{<0,j>,K+1} \right)^2$. Using the moment-generating function (MGF) approach, the average BER for the OSTBC with BFSK in MIMO-AF relaying can be upper-bounded as

$$P_e \leq \frac{1}{\pi} \int_0^{\frac{\pi}{2}} M_\gamma \left(\frac{g}{\sin^2 \theta} \right) d\theta \tag{44}$$

where $g = \frac{1}{2}$ for BFSK.

The MGF of $\hat{\gamma}_{<0,K+1>}^{<g>}$ and $\hat{\gamma}_{<j,K+1>}^n$ can be obtained as (see Appendix)

$$M_{\hat{\gamma}_{<0,K+1>}^{<g>}}(s) = \left(1 + \frac{E_0}{N_0} \left(\sigma_{<0,K+1>}^2 - \tilde{\sigma}_{<0,K+1>}^2 \right) \varepsilon_{<0,K+1>}^{<g>} s \right)^{-N_0} \tag{45}$$

$$M_{\hat{\gamma}_{<j,K+1>}^n}(s) = \begin{cases} \frac{\Gamma(N_0 - N_{K+1})}{\Gamma(N_0) \left(\frac{E_0}{N_0} \left(\beta_{<j>}^{<n>} \right)^2 \left(\sigma_{<0,j>,K+1}^2 - \tilde{\sigma}_{<0,j>,K+1}^2 \right) \varepsilon_{<j,K+1>}^{<n,g>} \right)^{N_{K+1}}}, & N_0 > N_{K+1} \\ \frac{\Gamma(N_{K+1} - N_0)}{\Gamma(N_{K+1}) \left(\frac{E_0}{N_0} \left(\beta_{<j>}^{<n>} \right)^2 \left(\sigma_{<0,j>,K+1}^2 - \tilde{\sigma}_{<0,j>,K+1}^2 \right) \varepsilon_{<j,K+1>}^{<n,g>} s \right)^{N_0}}, & N_0 < N_{K+1} \\ \frac{\log \left(\frac{E_0}{N_0} \left(\beta_{<j>}^{<n>} \right)^2 \left(\sigma_{<0,j>,K+1}^2 - \tilde{\sigma}_{<0,j>,K+1}^2 \right) \varepsilon_{<j,K+1>}^{<n,g>} s \right)}{\Gamma(N_{K+1}) \left(\frac{E_0}{N_0} \left(\beta_{<j>}^{<n>} \right)^2 \left(\sigma_{<0,j>,K+1}^2 - \tilde{\sigma}_{<0,j>,K+1}^2 \right) \varepsilon_{<j,K+1>}^{<n,g>} s \right)^{N_{K+1}}}, & N_0 = N_{K+1} \end{cases} \tag{46}$$

Since $\hat{\gamma}_{<0,K+1>}^{<g>}$ and $\hat{\gamma}_{<j,K+1>}^{<n>}$ are statistically independent, (44) can be written as

$$P_e \leq \frac{1}{\pi} \int_0^{\frac{\pi}{2}} \prod_{g=1}^{N_{K+1}} M_{\hat{\gamma}_{<0,K+1>}^{<g>}}(s) \left(\frac{g}{\sin^2 \theta} \right)^{j=K,n=N_j} \prod_{j=1,n=1} \quad (47)$$

$$M_{\hat{\gamma}_{<j,K+1>}^{<n>}}(s) \left(\frac{g}{\sin^2 \theta} \right) d\theta$$

One can obtain an upper-bound BER expression of the network by substituting (46) and (45) into (47). In the high SNR region, one of the key parameters to determine the system performance is diversity order. This parameter can be derived by using the upper-bound BER expression. Under the high SNR assumption, $\tilde{\sigma}_{<0,K+1>}^2$ ($i = 0, \dots, K$) and $\tilde{\sigma}_{<0,j,K+1>}^2$ ($i = 1, \dots, K$) approach 0. It then can be verified that a maximum diversity order of $N_0 N_{K+1} + \max\{N_0, N_{K+1}\} \sum_{j=1}^K N_j$ is achieved. For the case in which the source is equipped with two transmit antennas ($N_0 = 2$) while the multiple relays and destination are equipped with a single antenna ($N_1 = \dots = N_{K+1} = 1$), the maximum possible diversity order of the system is $K+2$, which is confirmed in [18-20]. When there is only one relay equipped with a single antenna in the network, the diversity order of the system is $N_{K+1} + N_0 N_{K+1}$ if $N_{K+1} < N_0$, which is the maximum possible diversity order of the considered MIMO AF relaying system.

4 Simulation results

This section presents simulation results for the performance of OSTBC transmission in MIMO AF relaying employing the proposed scheme. In conducting the simulations, it is assumed that the source and relays have an equal transmit power, i.e., $E_i = E$, $i = 0, \dots, K$. The noise components at the receivers, i.e., relays and destination, are modeled as i.i.d. $\mathcal{CN}(0, 1)$ random variables. The path loss follows the exponential decay model, i.e., $(\sigma_{<i,j>})^2 = d_{<i,j>}^{-\nu}$ where $d_{<i,j>}$ is the distance between node i and node j . All the simulations are reported with the path loss exponent $\nu = 4$. In addition, all the relays are assumed to have the same distances to the source and to the destination, i.e., $d_{0,1} = d_{0,2} = \dots = d_{0,K} = d_1$, $d_{1,K+1} = d_{2,K+1} = \dots = d_{K,K+1} = d_2$, and $d_{0,K+1} = d_0$. The Doppler frequencies are set as $10f_{0,i}T = f_{i,K+1}T = f_{0,K+1}T = 0.01$, $i = 1, \dots, K$. BFSK modulation is employed at the source.

Figure 2 shows the average BER of the proposed scheme by simulation for a single-relay network. In this setup, the source is equipped with two antennas, and the relay and destination are equipped with a single antenna. Naturally, an Alamouti space-time block code is used at the source. One can observe the tightness of the derived upper-bound BER of the proposed scheme. Also, the diversity order of 3 is confirmed^c.

Figure 3 presents the performance of the proposed scheme for a two-relay network in which all the nodes are equipped with two antennas. The relays are placed at the midpoint between the source and destination. Again, the source employs an Alamouti space-time block code to transmit the signal to the destination. It is observed from the figure that the performance gap between the proposed scheme and the coherent scheme decreases as P increases. For instance, the performance gap between the coherent scheme and the proposed scheme with $P = 0$ and with $P = 2$ at error probability 10^{-6} is about 6 and 3 dB, respectively. It is expected since additional (implicit) pilot symbols may improve the performance but will increase the complexity.

The BER performance of the proposed scheme and the coherent scheme is illustrated in Figure 4 for the case of a single-relay network in which the source is equipped with three antennas and the relay and destination are equipped with two antennas. The orthogonal space-time code for three transmit antennas is employed at the source [26]. In this simulation, the relays are placed close to the source. The figure again confirms that one can get the estimations of the (overall) channels in MIMO AF relaying networks employing the M -FSK modulation without the explicit pilot symbols to perform a detection. Note that the performance gap to the coherent scheme of the proposed scheme becomes smaller when P increases.

Finally, Figure 5 plots simulated BER performance of the proposed scheme and the coherent scheme for a single-relay network in which the source is equipped with three antennas and the relay and destination are equipped with two antennas. Again, the orthogonal space-time code for three transmit antennas is used at the source [26]. It can be seen from the figure that the BER performance of the proposed scheme and the coherent scheme degrades with increasing number of bits per symbol. However, the proposed scheme achieves a full diversity order with arbitrary values of M [13].

5 Conclusions

A detection scheme for MIMO AF relaying networks has been proposed. The investigated networks are composed of one source, K relays, and one destination. OSTBC is employed at the source together with M -ary FSK modulation to transmit the signals to the destination. By using the orthogonal property of FSK signaling, we have discussed an overall channel estimation method without the explicit pilot symbols. With the estimated overall channels, a maximal ratio combiner is employed to detect the transmitted information. An upper-bound expression on the probability of errors is obtained for a general network with K relays and arbitrary numbers of transceiver antennas at the source, relays, and destination. In addition, we have derived that the proposed detection scheme can achieve a

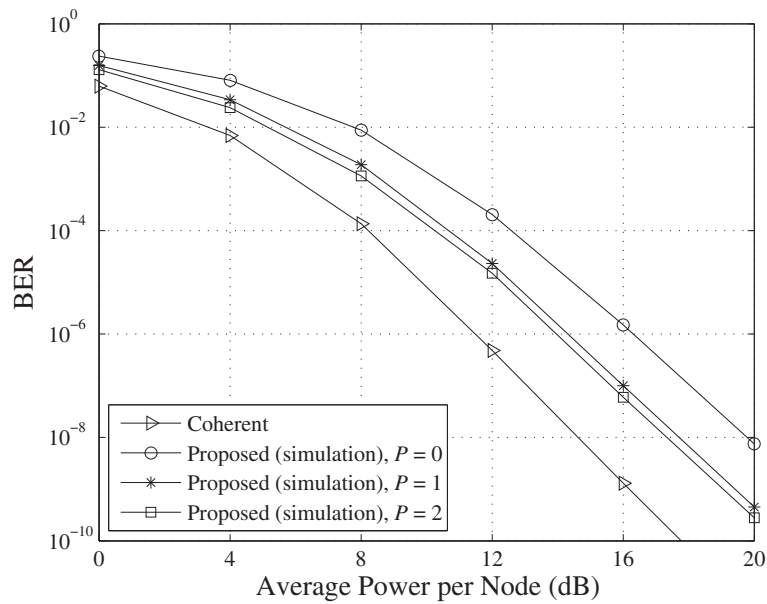


Figure 2 Error performance of a single-relay network with Alamouti space-time code. When $M = 2$ (BFSK), $N_0 = 2, N_1 = N_2 = 1$ (the source is equipped with two antennas, and the relay and destination are equipped with a single antenna), $d_0 = 0.8, d_1 = 1, d_2 = 1$.

full diversity order. Simulation results are also presented to validate the analytical results.

Endnote

^a Without loss of generality, the orthogonal channels are assumed to be made by means of time-division multiplexing.

^b Note that the index k is dropped for ease of notation.

^c To the best of our knowledge, there are no state-of-the-art non-coherent detectors for MIMO AF relaying to compare with our scheme. The coherent detector is the only work that is close to our work. Therefore, to verify our proposed scheme, comparison with the coherent detector is considered.

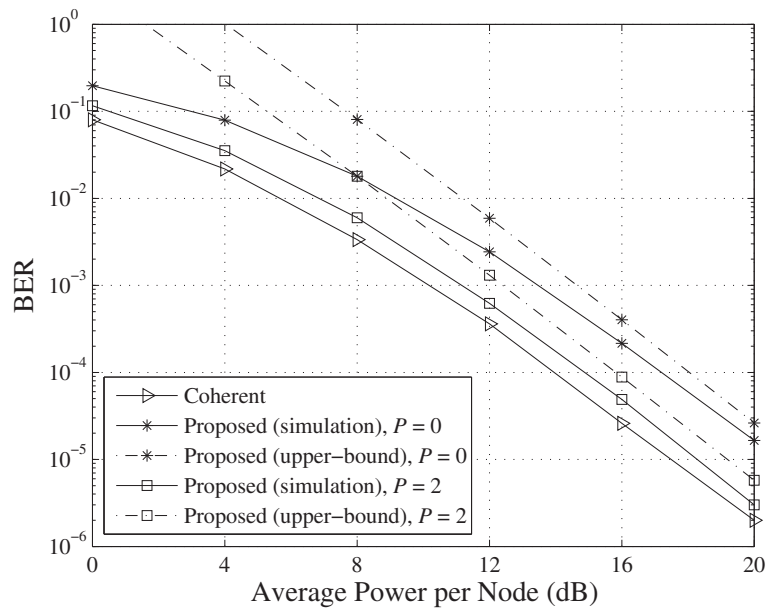


Figure 3 Error performance of a two-relay network with Alamouti space-time code. When $M = 2$ (BFSK), $N_0 = N_1 = N_2 = N_3$ (all the nodes are equipped with two antennas), $d_0 = 1, d_1 = 1, d_2 = 1$.

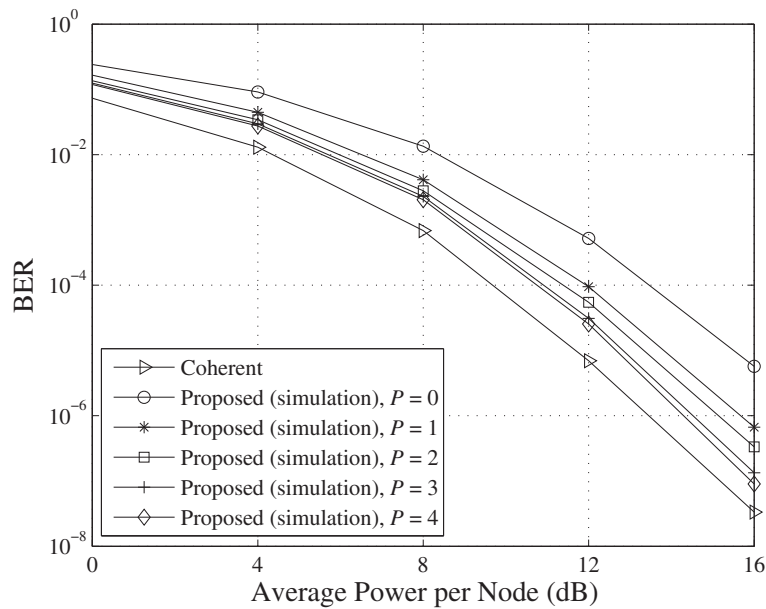


Figure 4 Error performance of a single-relay network with orthogonal space-time code. When $M = 2$ (BFSK), $N_0 = 3$, $N_1 = N_2 = 2$ (the source is equipped with three antennas, and the relay and destination are equipped with two antennas), $d_0 = 1$, $d_1 = 0.5$, $d_2 = 1.5$.

Appendix

Derivation of (46)

Let $Y = \sum_{g=1}^{N_{K+1}} \sum_{m=1}^{N_0} |\hat{h}_{<0,j,K+1>}^{<m,n,g>}|^2 = \left(\sum_{m=1}^{N_0} |\hat{h}_{<0,j>}^{<m,n>}|^2 \right) \left(\sum_{g=1}^{N_{K+1}} |\hat{h}_{<j,K+1>}^{<n,g>}|^2 \right) = X_1 X_2$ where $X_1 = \sum_{m=1}^{N_0} |\hat{h}_{<0,j>}^{<m,n>}|^2$ and $X_2 = \sum_{g=1}^{N_{K+1}} |\hat{h}_{<j,K+1>}^{<n,g>}|^2$.

Due to the fact that $|\hat{h}_{<0,j>}^{<m,n>}|$ and $|\hat{h}_{<j,K+1>}^{<n,g>}|$ are the estimates of $|h_{<0,j>}^{<m,n>}|$ and $|h_{<j,K+1>}^{<n,g>}|$, one can approximate that the pdfs of $|\hat{h}_{<0,j>}^{<m,n>}|$ and $|\hat{h}_{<j,K+1>}^{<n,g>}|$ have the same form as the pdfs of $|h_{<0,j>}^{<m,n>}|$ and $|h_{<j,K+1>}^{<n,g>}|$, respectively. Since $|h_{<0,j>}^{<m,n>}|$ and $|h_{<j,K+1>}^{<n,g>}|$ are Rayleigh

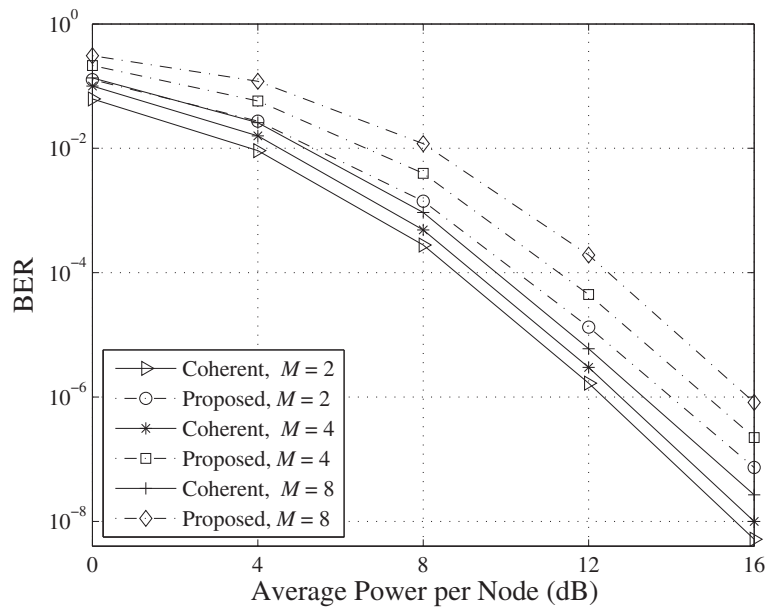


Figure 5 Error performance of a single-relay network with orthogonal space-time code. When $M = 2$, $M = 4$ and $M = 6$, $P = 2$, $N_0 = 3$, $N_1 = N_2 = 2$ (the source is equipped with three antennas, and the relay and destination are equipped with two antennas), $d_0 = d_1 = d_2 = 1$.

distributed, the pdfs of $\left| \hat{h}_{<0,j>}^{<m,n>} \right|$ and $\left| \hat{h}_{<j,K+1>}^{<n,g>} \right|$ can be approximated as $f_{\left| \hat{h}_{<0,j>}^{<m,n>} \right|^2}(x) = \frac{1}{\hat{\sigma}_{<0,j>}^2} e^{-\frac{x}{\hat{\sigma}_{<0,j>}^2}}$ and $f_{\left| \hat{h}_{<j,K+1>}^{<n,g>} \right|^2}(x) = \frac{1}{\hat{\sigma}_{<j,K+1>}^2} e^{-\frac{x}{\hat{\sigma}_{<j,K+1>}^2}}$, respectively. It is clear that X_1 and X_2 are chi-square random variables with $2N_0$ degrees of freedom with the pdf, respectively, as

$$f_{X_1}(x) = \frac{x^{N_0-1} e^{-\frac{x}{\hat{\sigma}_{<0,j>}^2}}}{(\hat{\sigma}_{<0,j>}^2)^{2N_0} \Gamma(N_0)}, \tag{48}$$

$$f_{X_2}(x) = \frac{x^{N_{K+1}-1} e^{-\frac{x}{\hat{\sigma}_{<j,K+1>}^2}}{(\hat{\sigma}_{<j,K+1>}^2)^{2N_{K+1}} \Gamma(N_{K+1})} \tag{49}$$

The MGF of Y can then be computed as follows [27,28]:

Case 1 ($N_0 > N_{K+1}$):

$$\begin{aligned} M_Y(s) &= \int_0^\infty f_{X_1}(x) M_{X_2}(sx) dx \\ &= \int_0^\infty \frac{x^{N_0-1} e^{-\frac{x}{\hat{\sigma}_{<0,j>}^2}}}{(\hat{\sigma}_{<0,j>}^2)^{2N_0} \Gamma(N_0)} \frac{1}{(1 + \hat{\sigma}_{<j,K+1>}^2 sx)^{N_{K+1}}} dx \\ &\simeq \int_0^\infty \frac{x^{N_0-N_{K+1}-1} e^{-\frac{x}{\hat{\sigma}_{<0,j>}^2}}}{\Gamma(N_0) (\hat{\sigma}_{<0,j>}^2)^{2N_0}} \frac{1}{(\hat{\sigma}_{<j,K+1>}^2)^{2N_{K+1}} s^{N_{K+1}}} dx \\ &= \frac{\Gamma(N_0 - N_{K+1}) (\hat{\sigma}_{<0,j>}^2)^{N_0 - N_{K+1}}}{\Gamma(N_0) (\hat{\sigma}_{<0,j>}^2)^{N_0} (\hat{\sigma}_{<j,K+1>}^2)^{2N_{K+1}} s} = \frac{\Gamma(N_0 - N_{K+1})}{\Gamma(N_0) \hat{\sigma}_{<0,j,K+1>}^{2N_{K+1}} s} \end{aligned} \tag{50}$$

Case 2 ($N_0 < N_{K+1}$): Similar to case 1, but N_0 and N_{K+1} are interchanged, one has

$$M_Y(s) = \frac{\Gamma(N_{K+1} - N_0)}{\Gamma(N_{K+1}) \hat{\sigma}_{<0,j,K+1>}^{2N_0} s} \tag{51}$$

Case 3 ($N_0 = N_{K+1}$): With $p = q + x$ where $q = \frac{1}{\hat{\sigma}_{<0,K+1>}^2 s}$ (8.350)

$$\begin{aligned} M_Y(s) &= \int_0^\infty \frac{x^{N_{K+1}-1} e^{-\frac{x}{\hat{\sigma}_{<j,K+1>}^2}}}{\Gamma(N_{K+1}) (\hat{\sigma}_{<j,K+1>}^2)^{2N_{K+1}}} \frac{1}{(1 + \hat{\sigma}_{<0,j>}^2 sx)^{N_0}} dx \\ &= \int_q^\infty \frac{(p-q)^{N_{K+1}-1} e^{-\frac{p-q}{\hat{\sigma}_{<j,K+1>}^2}}}{\Gamma(N_{K+1}) (\hat{\sigma}_{<j,K+1>}^2)^{2N_{K+1}}} \frac{q^{N_0}}{p^{N_0}} dp \\ &\simeq \int_q^\infty \frac{e^{-\frac{q}{\hat{\sigma}_{<j,K+1>}^2}} p^{-1} e^{-\frac{p}{\hat{\sigma}_{<j,K+1>}^2}}}{\Gamma(N_{K+1}) (\hat{\sigma}_{<0,j,K+1>}^2)^{2N_{K+1}} s^{N_{K+1}}} dp \\ &= \frac{1}{\Gamma(N_{K+1}) (\hat{\sigma}_{<0,j,K+1>}^2)^{2N_{K+1}} s^{N_{K+1}}} \frac{e^{-\frac{1}{\hat{\sigma}_{<0,j,K+1>}^2 s} \Gamma(0, 1/\hat{\sigma}_{<0,j,K+1>}^2 s)}}{\Gamma(N_{K+1}) (\hat{\sigma}_{<0,j,K+1>}^2)^{2N_{K+1}} s^{N_{K+1}}} \\ &= \frac{1}{\Gamma(N_{K+1}) (\hat{\sigma}_{<0,j,K+1>}^2)^{2N_{K+1}} s^{N_{K+1}}} \frac{e^{-\frac{1}{\hat{\sigma}_{<0,j,K+1>}^2 s} \Gamma(0, 1/\hat{\sigma}_{<0,j,K+1>}^2 s)}}{\Gamma(N_{K+1}) (\hat{\sigma}_{<0,j,K+1>}^2)^{2N_{K+1}} s^{N_{K+1}}} \\ &\leq \frac{\log \hat{\sigma}_{<0,j,K+1>}^2}{\Gamma(N_{K+1}) (\hat{\sigma}_{<0,j,K+1>}^2)^{2N_{K+1}} s^{N_{K+1}}} \end{aligned} \tag{52}$$

Competing interests

The authors declare that they have no competing interests.

Acknowledgements

This research is funded by the Vietnam National Foundation for Science and Technology Development (NAFOSTED) under grant number 102.04-2012.33.

Author details

¹School of Engineering, Tan Tao University, Tan Duc E-city, Duc Hoa, Long An, Vietnam. ²Singapore University of Technology and Design, Singapore, Singapore. ³Faculty of Electronics and Telecommunications, University of Science, Vietnam National University, Ho Chi Minh City, Vietnam.

Received: 7 May 2014 Accepted: 6 January 2015

Published online: 10 February 2015

References

1. A Sendonaris, E Erkip, B Aazhang, User cooperation diversity. Part I: System description. *IEEE Trans. Commun.* **51**(11), 1927–1938 (2003)
2. A Sendonaris, E Erkip, B Aazhang, User cooperation diversity. Part II: Implementation aspects and performance analysis. *IEEE Trans. Commun.* **51**(11), 1939–1948 (2003)
3. J Laneman, D Tse, G Wornell, Cooperative diversity in wireless networks: efficient protocols and outage behavior. *IEEE Trans. Inform. Theory.* **50**, 3062–3080 (2004)
4. J Laneman, G Wornell, Distributed space-time-coded protocols for exploiting cooperative diversity in wireless networks. *IEEE Trans. Inform. Theory.* **49**, 2415–2425 (2003)
5. T Himsoon, W Su, K Liu, Differential transmission for amplify-and-forward cooperative communications. *IEEE Signal Process. Lett.* **12**, 597–600 (2005)
6. T Himsoon, W Pam Siriwongpairat, W Su, K Liu, Differential modulations for multinode cooperative communications. *IEEE Trans. Signal Process.* **56**, 2941–2956 (2008)
7. Q Zhao, H Li, Differential modulation for cooperative wireless systems. *IEEE Trans. Signal Process.* **55**, 2273–2283 (2007)
8. Q Zhao, H Li, P Wang, Performance of cooperative relay with binary modulation in Nakagami- m fading channels. *IEEE Trans. Veh. Technol.* **57**, 3310–3315 (2008)
9. R Annavajjala, P Cosman, L Milstein, On the performance of optimum noncoherent amplify-and-forward reception for cooperative diversity. *Proc. IEEE Military Commun. Conf.* **5**, 3280–3288 (2005)
10. Y Zhu, P-Y Kam, Y Xin, Non-coherent detection for amplify-and-forward relay systems in a Rayleigh fading environment. *Proc. IEEE Global Telecommun. Conf.*, 1658–1662 (2007)
11. MR Souryal, Non-coherent amplify-and-forward generalized likelihood ratio test receiver. *IEEE Trans. Wireless Commun.* **9**, 2320–2327 (2010)
12. G Farhadi, N Beaulieu, A low complexity receiver for noncoherent amplify-and-forward cooperative systems. *IEEE Trans. Commun.* **58**, 2499–2504 (2010)
13. H Nguyen, H Nguyen, T Le-Ngoc, Amplify-and-forward relaying with M -FSK modulation and coherent detection. *IEEE Trans. Commun.* **60**, 1555–1562 (2012)
14. P Liu, S Gazor, I-M Kim, DI Kim, Noncoherent amplify-and-forward cooperative networks: robust detection and performance analysis. *IEEE Trans. Commun.* **61**, 3644–3659 (2013)
15. S Jin, M McKay, C Zhong, K-K Wong, Ergodic capacity analysis of amplify-and-forward MIMO dual-hop systems. *IEEE Trans. Inform. Theory.* **56**, 2204–2224 (2010)
16. Y Song, H Shin, E-K Hong, MIMO cooperative diversity with scalar-gain amplify-and-forward relaying. *IEEE Trans. Commun.* **57**, 1932–1938 (2009)
17. P Dharmawansa, M McKay, R Mallik, Analytical performance of amplify-and-forward MIMO relaying with orthogonal space-time block codes. *IEEE Trans. Commun.* **58**, 2147–2158 (2010)
18. H Muhaidat, M Uysal, Cooperative diversity with multiple-antenna nodes in fading relay channels. *IEEE Trans. Wireless Commun.* **7**, 3036–3046 (2008)
19. S Muhaidat, J Cavers, P Ho, Transparent amplify-and-forward relaying in MIMO relay channels. *IEEE Trans. Wireless Commun.* **9**, 3144–3154 (2010)
20. H Nguyen, H Nguyen, T Le-Ngoc, in *2012 Fourth International Conference on Communications and Electronics (ICCE)*. Wireless relay networks with

- Alamouti space-time code and M -FSK modulation (Hue, 1–3 August 2012), pp. 161–165
21. R Nabar, H Bolcskei, F Kneubuhler, Fading relay channels: performance limits and space-time signal design. *IEEE J. Select. Areas in Commun.* **22**, 1099–1109 (2004)
 22. P Ho, Z Songhua, KP Yuen, Space-time FSK: an implicit pilot symbol assisted modulation scheme. *IEEE Trans. Wireless Commun.* **6**, 2602–2611 (2007)
 23. C Patel, G Stuber, Channel estimation for amplify and forward relay based cooperation diversity systems. *IEEE Trans. Wireless Commun.* **6**, 2348–2356 (2007)
 24. B Gedik, M Uysal, Impact of imperfect channel estimation on the performance of amplify-and-forward relaying. *IEEE Trans. Wireless Commun.* **8**, 1468–1479 (2009)
 25. SM Kay, *Fundamentals of Statistical Signal Processing, Volume I: Estimation Theory*. (Prentice Hall, Upper Saddle River, 1998)
 26. H Jafarkhani, *Space-Time Coding: Theory and Practice*. (Cambridge University Press, Cambridge, 2005)
 27. JG Proakis, *Digital Communications*. (McGraw-Hill, New York, 2000)
 28. IS Gradshteyn, IM Ryzhik, A Jeffrey, D Zwillinger, *Table of Integrals, Series, and Products*. (Academic Press, Waltham, 2000)

Submit your manuscript to a SpringerOpen[®] journal and benefit from:

- ▶ Convenient online submission
- ▶ Rigorous peer review
- ▶ Immediate publication on acceptance
- ▶ Open access: articles freely available online
- ▶ High visibility within the field
- ▶ Retaining the copyright to your article

Submit your next manuscript at ▶ springeropen.com
